Positronium formation in poly(methyl methacrylate)

C. Dauwe,* B. Van Waeyenberge, and N. Balcaen

Department of Subatomic and Radiation Physics, Ghent University, Proeftuinstraat 86, B 9000 Ghent, Belgium
(Received 1 April 2003; published 3 October 2003)

Positron annihilation age momentum correlation (AMOC) experiments were performed in linear poly(methyl methacrylate), PMMA, at 420 K and 100 K. The lifetime and Doppler broadened line-shape $S(t)$ data were analyzed with Byakov and Stepanov's blob model for the formation of positronium. It is shown that the analysis is consistent with a delayed formation of positronium and also offers an alternative explanation for the observed broadening of the annihilation radiation line shape at short times (a few tens of picuseconds) after positron injection, the so called young age broadening.

The interpretation of positron annihilation data and of positronium formation in molecular liquids and solids, particularly in polymers, present some challenging riddles. Common lifetime spectra (LT) in polymers are analyzed as a composition of three exponential decay modes or components, indicated by their lifetimes $\tau_{1,2,3}$ and their intensities $I_{1,2,3}$. The shortest component is interpreted as due to the annihilation of parapositronium (p-Ps), the second component is due to annihilation of free positrons, and the longest one is the orthopositronium (o-Ps) component, where the intensity of the p-Ps component should be equal to one-third of the intensity of the o-Ps component. Such an interpretation is satisfactory if one is only interested in the o-Ps component and in the relation between $\tau_{o\text{-Ps}}$ and the mean size of the free-volume sites. Detailed analysis may lead to a number of discrepancies, given as follows.

(1) The lifetime of p-Ps, which is expected to be not very different from the lifetime in vacuum, i.e., 124 ps, has values as low as 100 ps or as high as 200 ps and its fitted intensity ratio to the long component is much higher than 1:3. Most authors dismiss these discrepancies as due to a complicated mixing of p-Ps with other unidentified states.

(2) The intensity of o-Ps, which has been believed to be related to the density of free-volume sites, is now known to depend on the chemical composition, the radiation[1,2] and mechanical[3] history of the sample, the electric field,[4] the polarity,[5] the content of electron-paramagnetic-resonance-active species,[6] and on bleaching by light.[7]

(3) In many cases the longest component splits up into two components. A number of possible explanations have been suggested, such as (i) the existence of two o-Ps states or of bound positron-ion states, (ii) the influence of slow trapping of the positronium into the free volume, and (iii) the existence of a broad distribution of the o-Ps lifetime.[8]

(4) The available AMOC (age momentum correlation) data on poly(methyl methacrylate) (PMMA)[9] and PE[10] have shown clearly that it is impossible to reproduce the time-dependent line-shape parameter $S(t)$ with the standard 3- or 4-component model.

In order to solve the foregoing problems it is necessary to establish a detailed model of positronium formation, particularly its evolution in time at the sub-nanosecond scale and to critically test this model for the AMOC experiments. We made the first attempt[9] by means of a model which supposes

that all Ps's are formed at $t=0$ and that they are slowly trapped into the free-volume sites. Both the lifetime spectrum and the $S(t)$ curve could be fitted well. However, there exist some problems which cause serious doubts on this slow trapping model. The first problem is that it was necessary to use different time-dependent functions for the lifetime and the $S(t)$ fittings. The second problem is related to the obtained mean trapping time $\tau=(0.54\pm0.04)$ ns. Because the lifetime of p-Ps is much shorter than its trapping time, this would mean that almost all p-Ps decays from the delocalized state, in which case the width of the angular correlation $\Delta\theta$ of p-Ps annihilations could not be used as a probe for the size of the trapping site. There exists overwhelming proof of the contrary, e.g., the papers of Jean and co-workers.[11,12]

The blob model for Ps formation was introduced by Byakov and Stepanov.[13] These authors concentrated on calculating the intensity of the long component, particularly its dependency on an applied electrical field, but they ignored the details of the sub-nanosecond behavior of positrons and the age-dependent formation of Ps. Therefore in this paper we will explore the performance of the blob model for a better understanding of the AMOC experiments in polymers. We have obtained experimental AMOC data at the Stuttgart pelletron positron beam[14] on a linear PMMA specimen at $T=100$ K and $T=420$ K. At each temperature 30 or more consecutive AMOC datasets of 1 h measuring time each were taken. The individual AMOC data were added up after we checked that there were no positron beam irradiation induced effects. Each summed set contains at least 2×10^7 counts. Summation of the data over the energy axis generates the overall experimental lifetime spectrum $\Lambda_{exp}(t)$ and the line-shape curve $S_{expt.}(t)$ is obtained by calculating the line-shape parameter for each time channel.

The essential elements of the "white" positron blob are as follows: a positron of several hundred keV will lose most of its energy within 10^{-11} s through ionizing collisions until its energy drops below the ionization threshold. In the final ionizing regime, with the positron energy between 0.5 keV and the ionization threshold, ≈30 electron-ion pairs are generated within a spherical volume called the blob. The subionizing positron further undergoes positron-phonon scattering and may diffuse out of the blob, until it becomes thermalized in a spherical volume bigger than the blob volume. Thus at zero time we consider a situation where (1) a number of free

electrons n_- are radially distributed around the blob center as a Gauss function $G(r)$ with dispersion σ_-, so the electron density is $\rho_-(r,t=0)=n_-(t=0)G(r)$ and $\int 4\pi r^2 G(r)dr=1$; (2) the initial positron density function $\rho_+(r,t=0)$ is also a Gauss function with dispersion $\sigma_+ > \sigma_-$; and (3) only positrons are present, positronium has still to be formed, $\rho_{p\text{-Ps}}(r,t=0)=\rho_{o\text{-Ps}}(r,t=0)=0$.

Subsequently for $t>0$ many changes occur, given as follows.

(i) According to a discussion by Stepanov[15] we assume that the blob electrons are confined to the blob by the attraction of the positive ions. This means that we may ignore blob expansion and assume that the electron distribution is approximately static, although the electrons still diffuse over small distances within the blob and recombine with the ions. We found that this recombination is reasonably described by an exponential decrease of the total number of free electrons $n_-(t)=n_-(0)\exp(-\kappa t)$, where $\tau_b=\kappa^{-1}$ is the blob recombination lifetime.

(ii) Free positrons undergo either direct annihilation with a decay constant λ_+, form positronium with any free or losely bound electron, and undergo spatial redistribution through diffusion. The formation of positronium at a time t, at position r, is proportional to the overlap of the blob electron and the positron density or $(d\rho_{\text{Ps}}/dt)_{form}=k\rho_-\rho_+$, where k is the chemical reaction constant for Ps formation, and the formation is distributed between p-Ps and o-Ps with the fixed ratio of 1/4 to 3/4. These processes are described by a set of rate equations;

$$\dot{\rho}_{p\text{-Ps}}(r,t)=\frac{1}{4}kn_-(t)G(r)\rho_+(r,t)-\lambda_{p\text{-Ps}}\rho_{p\text{-Ps}}(r,t),$$

$$\dot{\rho}_{o\text{-Ps}}(r,t)=\frac{3}{4}kn_-(t)G(r)\rho_+(r,t)-\lambda_{o\text{-Ps}}\rho_{o\text{-Ps}}(r,t), \quad (1)$$

$$\dot{\rho}_+(r,t)=-[kn_-(t)G(r)+\lambda_+]\rho_+(r,t)+D_+\nabla^2\rho_+(r,t).$$

When there is evidence of two or more Ps states j, Eqs. (1) are easily modified by splitting the formation constant k into $k^{(j)}$ and including also several decay constants $\lambda_{o\text{-Ps}}^{(j)}$. The resulting lifetime spectrum is $\Lambda(t)=\Sigma L_i(t)$, where the index i stands for p-Ps, free e^+, and one or more o-Ps states, and generally $L_i(t)=4\pi\lambda_i\int r^2\rho_i(r,t)dr$. The corresponding $S(t)$ curve is expressed as $S(t)=\Sigma S_i(t)L_i(t)/\Lambda(t)$. Generally, the $S_i(t)$ coefficients may be functions of the positron age t. However, if we assume that the Ps is formed in its final state, particularly that the trapping of Ps into the free-volume sites is immediate, then each contribution has a characteristic constant S_i value. Recently, Stepanov and Byakov[15] have found approximate analytical solutions to Eqs. (1), by integrating the o-Ps decay contribution over all positron ages. In order to avoid approximations and to keep the age dependency, we have calculated the different populations and activities by numerical evaluation, replacing the differentials by finite differences $\Delta r=3$ nm and $\Delta t=2.5$ ps and the Laplace operator $\nabla^2\rho_+$ by its finite equivalent $[\rho_+(r-\Delta r) -2\rho_+(r)+\rho_+(r+\Delta r)]/\Delta r^2 +[\rho_+(r+\Delta r)-\rho_+(r-\Delta r)]/(r\Delta r)$. As an illustration we have calculated the

TABLE I. Results of the blob analysis.

	PMMA at 100 K	PMMA at 420 K
σ_- (nm)	44	43
σ_+ (nm)	50	46
τ_b (ps)	25	31
D_+ (nm²/ns)	476	555
$\tau_{p\text{-Ps}}$ (ns)	0.124	0.138
τ_+ (ns)	0.328	0.331
$\tau_{o\text{-Ps}}^{(1)}$ (ns)	0.78	1.01
$\tau_{o\text{-Ps}}^{(2)}$ (ns)	1.75	2.62
$S_{p\text{-Ps}}$	0.640	0.669
S_+	0.509	0.509
$S_{o\text{-Ps}}^{(1)}$	0.506	0.529
$S_{o\text{-Ps}}^{(2)}$	0.525	0.528
$\chi_{t,s}^2$	0.94	0.97
$I_{\text{Ps}}^1(\%)$	9.9	12.6
$I_{\text{Ps}}^2(\%)$	30.4	34.1

relative contributions $L_i(t)/\Lambda(t)$ to the lifetime spectrum for the set of parameters which correspond to the analysis of the linear PMMA sample at 420 K, column 3 in Table I. These contributions are presented in Fig. 1 for the first 2 ns. One sees that at $t=0$ only free-positron decay is present and that the only contribution to the $S(t)$ curve will be S_+. There is a fast buildup of the contribution of parapositronium $S_{p\text{-Ps}}$, which reaches its maximum after about 0.05 ns, with a corresponding sharp decrease of the free-positron contribution. As $S_{p\text{-Ps}}>S_+$, this will lead to an increase of $S(t)$ during the first 50 ps. This buildingup of the p-Ps contribution is characteristic of a delayed formation of Ps which is an intrinsic consequence of the interaction of the positron with the blob. Thus an observed broadening of the line shape during the early few tens of picoseconds may be partly due to delayed Ps formation, and not necessarily entirely due to the thermalization of epithermal p-Ps as is generally accepted in the work of the Stuttgart group.[16,17] After ≈ 2 ns the longest o-Ps contribution with $S_{o\text{-Ps}}^{(2)}$ dominates the value of $S(t)$.
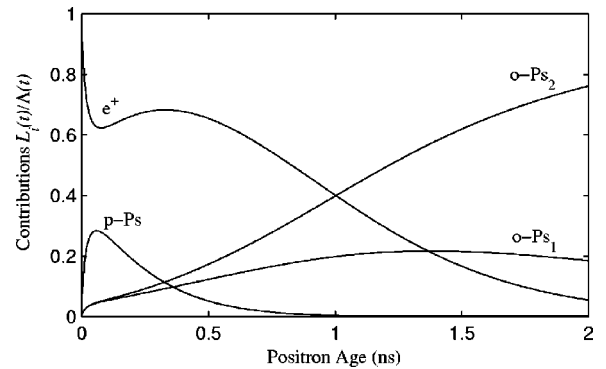

FIG. 1. Reconstruction of the relative contributions to the lifetime spectrum for linear PMMA at 420 K, presented before convolution with the time response function. These contributions correspond to the lifetime (not shown) and line-shape fittings shown in Fig. 2.
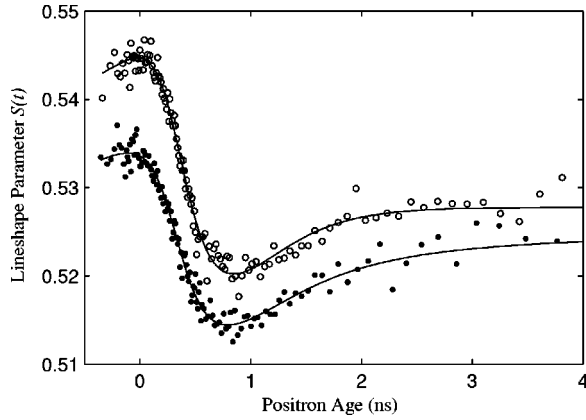
FIG. 2. Experimental $S(t)$ data of linear PMMA at 420 K (upper curve) and at 100 K (lower curve). The solid lines are the best fits obtained with the blob model, corresponding to the fitting parameters of Table I.

Therefore the effects of delayed formation of Ps are observable only in the first 2 ns, and they will not strongly interfere with the straightforward determination of the free-volume hole size by a multicomponent analysis. The numerical integration of Eqs. (1) was included into a Simplex based optimization procedure. Both the lifetime spectrum and the $S(t)$ curve were fitted simultaneously for the set of nonlinear parameters $[\sigma_-, \sigma_+, \kappa, D_+, k^{(1)}n_-(0), k^{(2)}n_-(0), \lambda_{p\text{-Ps}}, \lambda_+, \lambda_{o\text{-Ps}}^{(1)}, \lambda_{o\text{-Ps}}^{(2)}]$ and for the linear parameters $S_{p\text{-Ps}}$, S_+, $S_{o\text{-Ps}}^{(1)}$, and $S_{o\text{-Ps}}^{(2)}$.

The o-Ps component was split into two contributions, leading to the use of $k^{(1)}$ and $k^{(2)}$ and the two decay constants $\lambda_{o\text{-Ps}}^{(1)}$ and $\lambda_{o\text{-Ps}}^{(2)}$. Although the nature of the shorter o-Ps contribution is yet unidentified, we have considered that the two corresponding p-Ps contributions are undistinguishable. The $\chi_{t,s}^2$ of the fit is calculated from the deviations both in the LT and the S spectra:

$$\chi_{t,s}^2 = \frac{1}{2\nu_t} \sum_t \frac{[\Lambda(t_i) - \Lambda_{\text{expt.}}(t_i)]^2}{\Lambda_{\text{expt.}}(t_i)}$$
$$+ \frac{1}{2\nu_s} \sum \frac{[S(t_j) - S_{\text{expt.}}(t_j)]^2}{\sigma_s^2(t_j)}, \qquad (2)$$

where $\nu_t = n_t - 10$ and $\nu_s = n_s - 4$ are the number of degrees of freedom in the LT and the S fitting. The number of data points in the fitting regions are n_t and n_s. The $S(t)$ data were regrouped over the t axis in order to have at least 10^5 counts in each line-shape profile. This leads to $S(t)$ data which are unevenly spaced but which have constant standard deviations for higher positron ages. Figure 2 shows the experimental and fitted $S(t)$ curves at both temperatures. The obtained parameters are shown in Table I

The obtained blob size σ_- in linear PMMA is $\cong 43$ nm at both temperatures. We found no estimates in literature about the blob size in polymers to which our results could be compared. The available estimates of σ_- in some molecular liquids are in the range of 6.8–17.6 nm.[18] As expected, the size of the initial positron distribution σ_+ is about 10–20% big-

ger than σ_-. The order of magnitude of the blob lifetime τ_b is 25–31 ps. At this stage, and with the present statistics of the data, we cannot state if the difference between the values at 100 K and 420 K is significant. The fitted positron diffusion constants D_+ are very small. Positron diffusion constants in polymers, obtained from positron mobility measurements, vary over a wide range.[19,20] The lowest value was found for highly polar Kapton $D_+(\text{Kapton}) = 2.5$ nm^2/ns and probably the highest values are found in nonpolar polymers such as PE, where $D_+(\text{PE}) = 1.288 \times 10^5$ nm^2/ns at 399 K. Our fitted value of D_+ is a reasonable value for the polar PMMA specimen. Nagai *et al.*[21] have shown that the oxygen in poly(ethylene-vinyl acetate), E/VA, acts as a trap for positrons, which causes a strong reduction of the positron diffusion coefficient with respect to PE. This trapping site in E/VA is the acetate sequence O-C=O, which also occurs in the acrylate sidegroup of PMMA. The fitted values of the p-Ps lifetimes (124 ps and 138 ps) are close to the theoretical value of 124 ps for the free p-Ps. The small differences are caused by different pick-off annihilation rates and contact densities of the electron-positron pair in trapped p-Ps. The lifetimes of the longest o-Ps components, $\tau_{o\text{-Ps}}^{(2)}$ are in agreement with o-Ps trapped into the free volume sites, i.e., upon applying the well known Tao-Eldrup formula we find the radius of $R = 2.60$ Å in the glass state at 100 K and $R = 3.36$ Å in the rubber state at 420 K.

The nature of the shorter o-Ps component $\tau_{o\text{-Ps}}^{(1)}$ is still enigmatic. If two types of free or loosely bound electrons are present in the blob, or if the electrons are in different chemical environments, the two distinct Ps states may be formed. The lifetimes $\tau_{o\text{-Ps}}^{(1)}$ are too short to be Ps trapped into free-volume sites. Possibly they are states of Ps bound to molecules or shallowly trapped in the dipolar fields. Concerning the fitted S parameters, the values for free positrons S_+ are independent of temperature, while the S parameter of trapped o-Ps, $S_{o\text{-Ps}}^{(2)}$ is slightly bigger at 420 K than at 100 K. This slight increase is due to the lower kinetic energy of the trapped Ps in the free-volume sites at 420 K, and hence less penetration into the core electronic shells of the atoms in the free-volume walls. One can also estimate the free-volume sizes from the S parameters of p-Ps. We consider the p-Ps annihilation line to be Gaussian with an effective dispersion $\sigma^2 = \sigma_0^2 + \sigma_E^2$, where $\sigma_0 = 0.681$ keV is the instrumental energy dispersion of the Ge detector and σ_E is the intrinsic energy dispersion of the p-Ps peak. The relation between σ and S is $S_{p\text{-Ps}} = \text{erf}(d/2\sqrt{2}\sigma)$, where d is the width of the central part of the annihilation line which is used for the calculation of S. The radius of the free-volume site is $R(\text{Å}) \cong 1.80\sigma_E^{-1}$ (keV).[22] The resulting values are $R = 2.57$ Å at 100 K and $R = 2.92$ Å at 420 K, which correspond fairly well with the values obtained from the longest o-Ps lifetimes.

The total Ps fractions I_{Ps}^i are not fitted in the blob analysis, but they are obtained by an *a posteriori* integration of the different contributions, which depend on all other fitting parameters, but most strongly on the Ps formation rates $k^{(i)}n_-(0)$. Therefore we have shown I_{Ps}^i in Table I rather than the the Ps formation rates.
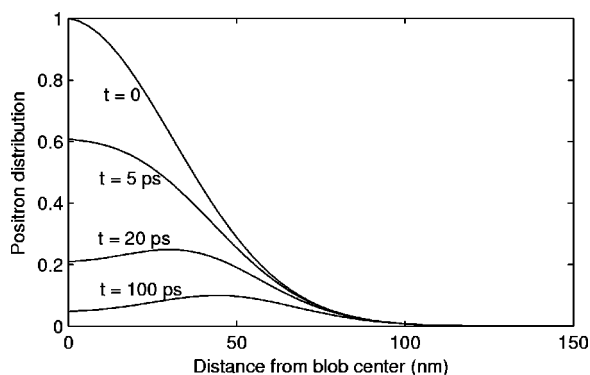
FIG. 3. Simulation of the time evolution of the positron distribution including positronium formation, free-positron decay, and positron diffusion. The parameters used are the fitted values from Table I corresponding to the PMMA at 420 K.

In Fig. 3 we show the time evolution of the positron density as calculated from the parameters which correspond to the analysis at 420 K. At $t=0$ both blob electron and positron distributions are Gaussian, the overlap between these two, and thus the Ps formation rate, is high in the center of the blob, and decreases with increasing distance from the center. The positron density is rapidly depleted in the center, leading to an off-center distribution which by the diffusion process reinjects positrons into the higher electron concentration zone of the blob. This behavior seems to be in agreement with the black blob model which is used by Ref. 15 in order to reproduce the variation of I_{Ps} with electrical field in molecular liquids. In the black blob model it is assumed that a central part of the positrons are bound inside the blob by the polarization of the electrons, which means that there is an "inside" part of the blob from which the positron cannot escape.

As a conclusion, we have shown that the blob model for positronium formation gives an adequate interpretation of AMOC data recorded in linear PMMA at two temperatures. It involves delayed formation of positronium and explains the young age broadening. The intensity of the o-Ps contribution does not depend on the quantity of free volume, but it is a complicated function of the blob chemistry. It is also shown that the corrections introduced in the black blob model may already be included in a properly coded white blob model.

*Electronic address: carlos.dauwe@rug.ac.be

[1] F. Maurer, Macromol. Symp. **83**, 205 (1994).

[2] V. Shantarovich, T. Hirade, I. Kevdina, V. Gustov, and M. Arzhakov, Mater. Sci. Forum **363-365**, 352 (2001).

[3] C. Wang, B. Wang, S. Li, and S. Wang, J. Phys.: Condens. Matter **5**, 7515 (1993).

[4] C. Wang, K. Hirata, J. Kawahara, and Y. Kobayashi, Phys. Rev. B **58**, 14 864 (1998).

[5] C. Qi, C. Wei, Y. Wu, S. Zhang, H. Wang, H. Li, T. Wang, and F. Yan, J. Polym. Sci., Part B: Polym. Phys. **38**, 435 (2000).

[6] T. Hirade, F. Maurer, and M. Eldrup, Radiat. Phys. Chem. **58**, 465 (2000).

[7] J. Zrubcova, J. Kristiak, W. Pedersen, and M. Eldrup, Mater. Sci. Forum **363-365**, 359 (2001).

[8] G. Dlubek and S. Eichler, Phys. Status Solidi A **168**, 333 (1998).

[9] C. Dauwe, N. Balcaen, B.V. Waeyenberge, S.V. Petegem, and H. Stoll, Mater. Sci. Forum **363-365**, 254 (2001).

[10] N. Suzuki, T. Hirade, F. Saito, and T. Hyodo, Radiat Phys. Chem. (in press).

[11] Y. Jean, Nucl. Instrum. Methods Phys. Res. B **56-57**, 615 (1991).

[12] Y. Jean, Y. Rhee, Y. Lou, D. Shelby, and G. Wilkes, J. Polym. Sci., Part B: Polym. Phys. **34**, 2979 (1996).

[13] V.M. Byakov and S.V. Stepanov, J. Radioanal. Nucl. Chem. **210**, 371 (1996).

[14] H. Stoll, M. Koch, K. Maier, and J. Major, Nucl. Instrum. Methods Phys. Res. B **56**, 582 (1991).

[15] S.V. Stepanov and V.M. Byakov, *Principles and Applications of Positron and Positronium Chemistry* (World Scientific, Singapore, 2003), Chap. 5.

[16] H. Stoll, P. Castellaz, S. Koch, J. Major, H. Schneider, A. Seeger, and A. Siegle, Mater. Sci. Forum **255-257**, 92 (1997).

[17] H. Schneider, A. Seeger, A. Siegle, H. Stoll, P. Castellaz, and J. Major, Appl. Surf. Sci. **116**, 145 (1997).

[18] S.V. Stepanov, V.M. Byakov, C.-L. Wang, Y. Kobayashi, and K. Hirata, Mater. Sci. Forum **363-365**, 392 (2000).

[19] R.S. Brusa, M.D. Naia, D. Margoni, and A. Zecca, Appl. Phys. A: Mater. Sci. Process. **60**, 447 (1995).

[20] R.S. Brusa, A. Dupasquier, E. Galvanetto, and A. Zecca, Appl. Phys. A: Solids Surf. **54**, 233 (1992).

[21] Y. Nagai, T. Nonaka, M. Hasegawa, Y. Kobayashi, C. Wang, W. Zheng, and C. Zhang, Phys. Rev. B **60**, 11 863 (1999).

[22] H. Nakanishi and Y. Jean, *Positron and Positrionium Chemistry* (Elsevier, New York, 1988), Chap. 6, p. 176.